

# Effect of dynamical asymmetry on the viscosity of a random copolymer melt

V. Kumaran

*Department of Chemical Engineering, Indian Institute of Science, Bangalore 560 012, India*

(Received 12 July 1995; accepted 2 November 1995)

The variation of the viscosity as a function of the sequence distribution in an  $A-B$  random copolymer melt is determined. The parameters that characterize the random copolymer are the fraction of  $A$  monomers  $f$ , the parameter  $\lambda$  which determines the correlation in the monomer identities along a chain and the Flory chi parameter  $\chi_F$  which determines the strength of the enthalpic repulsion between monomers of type  $A$  and  $B$ . For  $\lambda > 0$ , there is a greater probability of finding like monomers at adjacent positions along the chain, and for  $\lambda < 0$  unlike monomers are more likely to be adjacent to each other. The traditional Markov model for the random copolymer melt is altered to remove ultraviolet divergences in the equations for the renormalized viscosity, and the phase diagram for the modified model has a binary fluid type transition for  $\lambda > 0$  and does not exhibit a phase transition for  $\lambda < 0$ . A mode coupling analysis is used to determine the renormalization of the viscosity due to the dependence of the bare viscosity on the local concentration field. Due to the dissipative nature of the coupling, there are nonlinearities both in the transport equation and in the noise correlation. The concentration dependence of the transport coefficient presents additional difficulties in the formulation due to the Ito–Stratonovich dilemma, and there is some ambiguity about the choice of the concentration to be used while calculating the noise correlation. In the Appendix, it is shown using a diagrammatic perturbation analysis that the Ito prescription for the calculation of the transport coefficient, when coupled with a causal discretization scheme, provides a consistent formulation that satisfies stationarity and the fluctuation dissipation theorem. This functional integral formalism is used in the present analysis, and consistency is verified for the present problem as well. The upper critical dimension for this type of renormalization is 2, and so there is no divergence in the viscosity in the vicinity of a critical point. The results indicate that there is a systematic dependence of the viscosity on  $\lambda$  and  $\chi_F$ . The fluctuations tend to increase the viscosity for  $\lambda < 0$ , and decrease the viscosity for  $\lambda > 0$ , and an increase in  $\chi_F$  tends to decrease the viscosity. © 1996 American Institute of Physics. [S0021-9606(96)50506-0]

## I. INTRODUCTION

There have been many studies of the thermodynamics and dynamics of polymer melts in which the polymers contain two or more types of monomers. The interest stems not just from their practical applications, but also from the novel structures that could be formed by these polymer mixtures under certain conditions. The earlier studies<sup>1–3</sup> focused on the thermodynamics and dynamics of “homopolymers” which consisted of a mixture of two different type of polymers. There is a certain temperature below which these mixtures undergo a demixing transition, and the transition temperature is determined by a balance between the entropic effects which favor mixing and the enthalpic interactions which favor segregation of the monomers. The dynamics of early stage phase separation has been analyzed<sup>1–3</sup> using a treatment similar to the mean field Cahn–Hilliard<sup>4–6</sup> theory for spinodal decomposition, and there has also been some recent work on the adapting the Langer–Baron–Miller theory,<sup>7</sup> which includes nonlinear effects, for polymer mixtures. The late stage growth kinetics (Oswald ripening) of homopolymer mixtures has also been studied.<sup>1,2</sup>

In the recent years, there has been much work on copolymeric materials with well defined structures, such as block and star copolymers. These are prepared by anionic

polymerization of a mixture of “prepolymers” each of which consists of different monomers. The phase separation of copolymers is very different from that of homopolymers, because the different types of monomers are chemically linked on the same chain. As a result, they form “microphases” each of which is rich in one type of monomer. The shape of these microphases depends on the composition  $f$  (overall fraction of one of the monomers), and various microstructures<sup>8</sup> such as lamellar, cylindrical, spherical and ordered bicontinuous double diamond have been identified. The phase diagram for block copolymers has been studied in two limiting cases. In the weak segregation limit where,<sup>9,10</sup> the interaction between the monomers is sufficiently weak that the conformation of the individual polymers is not much disturbed, and the fluctuations about the mean concentration are small. In this limit, the composition fluctuation is approximately sinusoidal, and the period of the microdomains scales as  $N^{-1/2}$ , where  $N$  degree of polymerization. In the strong segregation limit,<sup>11,12</sup> narrow interfaces separate microdomains which are nearly pure in the two different types of monomers, and the polymer conformation is significantly perturbed from the equilibrium Gaussian shape. The renormalization of the transport coefficient near the order–disorder transition has been studied,<sup>13</sup> and the diffusion of

polymers in the ordered phases has also been analyzed.<sup>14</sup>

There has been relatively less work on random copolymers, where each polymer contains two different types of monomers  $A$  and  $B$  distributed stochastically along a chain.<sup>15–17</sup> In addition to the volume fraction of type  $A$  monomers  $f$  and the Flory chi parameter  $\chi_F$ , which represents the strength of the enthalpic repulsion between monomers  $A$  and  $B$ , the phase diagram depends on a parameter  $\lambda$  which represents the correlation between the identities of the monomers along the chain. The case  $\lambda = -1$  corresponds to an alternating copolymer, where the monomers  $A$  and  $B$  alternate along the chain, while the limit  $\lambda = 1$  corresponds to a mixture of homopolymers of type  $A$  and  $B$ . The intermediate value  $\lambda = 0$  represents a truly random copolymer, where  $A$  and  $B$  are distributed at random along a chain. Fredrickson, Milner, and Leibler<sup>17</sup> (FML) have shown that the phase diagram for this system has a complex dependence on the parameter  $\lambda$ , with a Lifshitz multicritical point at a value  $\lambda = \lambda_L$ . The value  $\lambda_L$  depends on the microscopic model, but is usually less than zero. For  $\lambda > \lambda_L$ , the transition is of the binary fluid type and the two coexisting phases have a composition difference proportional to  $O(N^{-1/2})$ . For  $\lambda < \lambda_L$ , the phase separation occurs at a finite wavelength, and is of the “microphase separation” type observed in block copolymers.

The anomalous behaviour of the transport coefficients in the vicinity of a critical point was analyzed by Kumaran and Fredrickson<sup>18</sup> (KF). The dynamical equations for the melt were similar to the Model H equations<sup>19,20</sup> used for studying the critical dynamics of binary fluids. The divergence in the Onsager coefficient and viscosity were determined as a function of the reduced temperature  $\epsilon = (T - T_c)/T_c$ , the fraction of  $A$  monomers  $f$  and the parameter  $\lambda$ . Here,  $T_c$  is the critical temperature. It was found that for  $\lambda < \lambda_L$ , the viscosity diverges proportional to  $\epsilon^{-3/2}$  near the critical point while the Onsager coefficient remains finite. In the limit  $\lambda > \lambda_L$ , the divergence in the viscosity is weak while the Onsager coefficient diverges proportional to  $\epsilon^{-1/2}$  for  $\epsilon^{-1}(\lambda - \lambda_L) \gg 1$ , and proportional to  $\epsilon^{-3/4}$  for  $\epsilon^{-1}(\lambda - \lambda_L) \ll 1$ .

The above critical dynamics studies have focused on the anomalous behavior of the transport coefficient near a critical point. Here, the nonlinear effects originate from the convective terms in the conservation equation, and the effect of these terms becomes significant only as the critical point is approached. Here, we study another type of viscosity renormalization in a random copolymer, which is due to the dependence of the viscosity on the local concentration. The dependence of the viscosity renormalization on the sequence distribution of the random copolymer is analyzed. This could be of use in polymer processing applications, where the kinetics of the polymerization reaction could be adjusted to obtain a copolymer whose viscosity is suitable for further processing.

In the present study, the mode coupling technique is used to study the effect of fluctuations in the concentration and velocity fields on the viscosity. Since the local fluctuations are related to the sequence distribution in the random copolymer, this effectively provides the variation in the viscosity as a function of the correlation in the monomer identities along

the chain. The type of nonlinearity considered here is present when the two polymers  $A$  and  $B$  have very different viscosities in the pure form, so that the viscosity of the mixture depends on the local concentration. This causes a “dissipative” nonlinearity in the conservation equations, since the diffusion coefficient in the Fokker–Planck equation for the probability distribution depends on the concentration. This is in contrast to the conservative nonlinearity, which originates from the convective streaming term in the Fokker–Planck equation. In addition, the upper critical dimension for the dissipative nonlinearity studied here is 2, in contrast to the upper critical dimension of 4 for the convective nonlinearity near a critical point. Therefore, the renormalization of the viscosity is convergent near a critical point, and could be important even at temperatures higher than the critical temperature.

The renormalization in the viscosity is determined using the Martin–Siggia–Rose functional integral formalism for the coupled Langevin equations for the concentration and velocity fields, which has been used earlier for the study of critical dynamics in simple fluids.<sup>19,20</sup> However, there are some additional difficulties encountered due to the dissipative nature of the nonlinearity. The correlation of the random noise in the distribution function is related to the diffusion coefficient for the probability distribution in the Fokker–Planck equation. The dependence of the diffusion coefficient on the concentration causes some ambiguity in the determination of the noise correlation. Since the noise correlation is assumed to be a delta function in time, the concentration field varies as a step function. Therefore, there is some ambiguity about whether the value of the concentration in the noise correlation is before or after the step, and this is called the Ito–Stratonovich paradox.<sup>21,22</sup> If the noise correlation is incorrectly chosen, certain inconsistencies may arise in the results; in particular, the stationarity condition and the fluctuation dissipation theorem may not be satisfied. This issue is considered in the Appendix, and it is found that the choice of noise correlation depends on the discretization scheme in the functional integral formulation. If the causal discretization is used, then it is appropriate to use the value of the noise correlation before the step change (Ito formulation). In the present analysis, the Ito formulation is used in conjunction with the causal discretization scheme, and it is also explicitly verified that the fluctuation dissipation theorem is satisfied.

The model for the random copolymer is presented in the next section. This is very similar to that used by FML and KF, though a minor modification is made to remove high wave number divergences in the wave vector integrals for the structure factor. The renormalization of the viscosity is calculated using a functional integral formalism in Sec. III, and the main conclusions are briefly summarized in Sec. IV.

## II. MODEL

The system consists of an incompressible random copolymer melt containing two type of monomers  $A$  and  $B$  in which the volumes of the monomers maintain a constant value  $v$ . The polymers are considered to be monodisperse,

each polymer contains  $\mathcal{N}_m$  monomers, and the volume fraction of type  $A$  monomers is  $f$ . The location of monomers along a chain are indexed by lower case indices  $n, m, \dots$  while the different chains are identified by upper case indices  $N, M, \dots$ . The correlation between the monomer identities at different separations along the chain is obtained from the Markov model of random copolymerization<sup>23</sup> which was earlier used by FML<sup>17</sup> and KF.<sup>18</sup> In this model, the reactivity of a monomer and a polymer chain depends only on the identities of the monomer located at the end of the polymer and the unreacted monomer itself, and four rate constants  $k_{KL} (\{K, L\} = A, B)$  are sufficient to determine the growth kinetics. In addition, it is usually assumed that the monomer concentrations are constant during the polymerization process.

The correlation of monomer identities along a chain can be expressed in terms of a conditional probability matrix  $p_{KL} (\{K, L\} = A, B)$ , which is the probability that a monomer of type  $L$  is followed by a monomer of type  $K$ . These probabilities follow two conservation conditions:

$$p_{AA} + p_{BA} = 1, \quad p_{AB} + p_{BB} = 1, \quad (1)$$

and a third relationship can be obtained from the condition that the relative concentrations of the two monomers remains a constant during polymerization

$$f = p_{AA}f + p_{AB}(1 - f). \quad (2)$$

Using these three relations, the correlation in the identity of the monomers can be expressed as a function of two parameters, i.e., the volume fraction  $f$ , and the nontrivial eigenvalue of the  $p_{KL}$  matrix  $\lambda$ , given by

$$\lambda = p_{AA} + p_{BB} - 1. \quad (3)$$

The parameter  $\lambda$  is a measure of the correlation in the monomer identities along a chain. In the limit  $\lambda = 1$ , the probabilities  $p_{AA}$  and  $p_{BB}$  are 1, indicating that a monomer of type  $A$  is followed only by another of type  $A$ , and similarly for  $B$ , producing a mixture of homopolymers of  $A$  and  $B$ . In the limit  $\lambda = -1$ , every monomer of type  $A$  is followed by one of type  $B$ , and vice versa, producing an alternating polymer. The case  $\lambda = 0$  represents an ideal random copolymer, where it is equally probable for a monomer of type  $A$  to be followed by type  $A$  or  $B$  monomers. In general, the polymer melt consists of chains that differ in composition and sequence distribution, and except in the limiting cases  $\lambda = 1$  and  $\lambda = -1$ , there is no correlation between the identities of monomers at a the same location on different chains. This is in contrast ordered systems such as block copolymers, where the identities of monomers on different chains are perfectly correlated.

The monomer sequence distribution can be conveniently expressed in terms of a random variable  $\theta(n, N)$ , which is  $+1$  if the monomer at position  $n$  on chain  $N$  is type  $A$ , and  $-1$  if the monomer at position  $n$  on chain  $N$  is type  $B$ . The moments of the variable  $\theta$  can be derived using the Markov model for copolymerization described above. The calculation of the structure factor requires the first two moments of the variable  $\theta$ , which are derived in FML<sup>17</sup>

$$\begin{aligned} \overline{\theta(n, N)} &= 2f - 1, \\ \overline{[\theta(n, N) - \theta(n, N)][\theta(m, M) - \theta(m, M)]} \\ &= 4f(1 - f)\lambda^{|n-m|}\delta_{NM}, \end{aligned} \quad (4)$$

where the overbars represent averages over the sequence distribution.

The microscopic densities of  $A$  and  $B$  monomers at a position  $\mathbf{x}$  and time  $t$  are given by

$$\phi_A(\mathbf{x}, t) = \sum_{N=1}^{\mathcal{N}_p} \sum_{n=1}^{\mathcal{N}_m} \left( \phi(n, N; \mathbf{x}, t) \frac{(1 + \theta(n, N))}{2} \right), \quad (5)$$

$$\phi_B(\mathbf{x}, t) = \sum_{N=1}^{\mathcal{N}_p} \sum_{n=1}^{\mathcal{N}_m} \left( \phi(n, N; \mathbf{x}, t) \frac{(1 - \theta(n, N))}{2} \right), \quad (6)$$

where the microscopic density field  $\phi(n, N; \mathbf{x}, t)$  of a monomer at position  $n$  on chain  $N$  is

$$\phi(n, N; \mathbf{x}, t) = \delta(\mathbf{x} - \mathbf{R}(n, N, t)) \quad (7)$$

and  $\mathbf{R}(n, N, t)$  is the monomer position. The interaction between the monomers is expressed using the Flory chi parameter which is an enthalpy penalty per monomer for  $A-B$  contacts relative to  $A-A$  and  $B-B$  contacts. The Hamiltonian is the standard Edwards Hamiltonian modified to account for enthalpic interactions

$$\begin{aligned} H &= \frac{3}{2b^2} \sum_{N=1}^{\mathcal{N}_p} \sum_{n=1}^{\mathcal{N}_m} |\mathbf{R}(n, N) - \mathbf{R}(n+1, N)|^2 \\ &+ \int_{\mathbf{k}} \phi_A(-\mathbf{k}) \chi_F(\mathbf{k}) \phi_B(\mathbf{k}), \end{aligned} \quad (8)$$

where  $\int_{\mathbf{k}} \equiv (2\pi)^{-3} \int d\mathbf{k}$ . Here,  $b$  is the statistical segment length of a monomer and  $\chi_F(\mathbf{k})$  is the nonlocal Flory interaction parameter. This is related to the usual Flory chi parameter by  $\chi_F = (\chi/v)(b/\sqrt{6})^3$ . In addition to the enthalpic interaction, there is the incompressibility condition which states that the sum of the monomer densities is a constant in the melt. This condition is enforced using the random phase approximation.

For a melt of ideal chains in the absence of interactions, the equilibrium pair distribution is a Gaussian distribution<sup>24</sup> which is given by

$$S_0(n, N; m, M; \mathbf{k}) = \frac{1}{V} \exp(-|n-m|k^2) \delta_{NM}. \quad (9)$$

Here, the wave vector  $k$  has been scaled by  $(\sqrt{6}/b)$ , where  $b$  is the statistical segment length of the monomers. There are deviations from this behavior due to two reasons—the interactions between the monomers which is represented by the Flory chi parameter  $\chi_F$ , and the incompressibility condition which requires a constant density in the melt. The incompressibility condition is enforced using the random phase approximation, where an external potential  $U(\mathbf{k}, \omega)$  is applied on the monomers to maintain constant density, and this potential is determined in terms of the concentrations in a self-consistent manner. The details of the calculation are given in

KF, and the effective structure factor which includes the effect of the hardcore repulsions which render the melt incompressible is

$$S'(\mathbf{k}) = \frac{1}{4} \sum_{n,N,m,M} S_0(n,N;m,M;\mathbf{k}) \times \frac{1}{[\theta(n,N) - \theta(n,N)][\theta(m,M) - \theta(m,M)]}. \quad (10)$$

At this point, we make a modification to the structure factor used in earlier studies<sup>17,18</sup> to avoid difficulties with divergent integrals later on. The above structure factor consists of two components—the self-component due to the perfect correlation in the identity of a single monomer at  $n=m$ , and the distinct component ( $n \neq m$ ) due to the correlation in the identities of different monomers located close together on the same chain. The self-component causes ultraviolet divergences in the convolution integrals over the wave vector, since it does not decay to zero for large  $k$ . One method to get around this difficulty is to use a large  $k$  (ultraviolet) cutoff  $k_{\max}$  which is of the same magnitude as the inverse of the segment length. In the present study, an alternative easier method is used. Since the dynamical nonidealities are due to the correlations between different monomers, the self-component is neglected while calculating the structure factor. This serves the same purpose as the ultraviolet cutoff, since it removes from the integrals contributions due to correlations over lengths smaller than the segment length. In addition, this formulation is also more realistic, because the thermodynamic and dynamical assymetries are due to the interactions between different monomers mediated by the correlation in their identities, and not due to the interaction of a monomer with itself. With this modification, the structure factor (10) which includes the effect of hardcore repulsions but not the enthalpic interactions, is

$$S'(\mathbf{k}) = 2f(1-f) \frac{\lambda \exp(-k^2)}{1 - \lambda \exp(-k^2)}, \quad (11)$$

where Eq. (4) has been used for the moments of  $\theta(n,N)$  in Eq. (10), and we have assumed, following KF, that  $\lambda \mathcal{N}^m \ll 1$ , i.e., the number of monomers in the polymer is sufficiently large that there is no correlation in the monomers located at the ends of the chain. This structure factor is different from the Debye-like function for homopolymers and block copolymers, because it lacks a correlation hole at the origin. In block copolymers, the identities of monomers located at identical positions on different chains are correlated, and so if a monomer at position  $n$  on chain  $N$  is located at the origin, the probability of finding another monomer at position  $n$  on chain  $M$  is reduced. However, in a random copolymer the identities of the species at position  $n$  on different chains are uncorrelated, and so there is no correlation hole in the structure factor. Due to the lack of correlation in the identities of monomers on different chains, the contribution to the structure factor due to the potential used to enforce incompressibility turns out to be  $O(1/\mathcal{N}_p)$  smaller than

the contribution due to the correlation in the monomers along a single chain, and so the latter provides the dominant contribution to the structure factor.

The structure factor which takes into account enthalpic interactions can be easily calculated from the above<sup>18</sup>

$$S(\mathbf{k}) = \frac{S'(\mathbf{k})}{1 - 2\chi_F S'(\mathbf{k})}. \quad (12)$$

Since the form of the structure factor [Eqs. (11) and (12)] used here is different from FML<sup>17</sup> and KF,<sup>18</sup> the phase behavior of the present model is also different. The present model predicts a phase transition only for  $\lambda > 0$ , and the transition temperature is given by  $\chi = f(1-f)(1-\lambda)/4\lambda$ . The most unstable mode has a wave number  $k=0$ , indicating that the transition is of the binary fluid type. For  $\lambda < 0$ , there is no transition in the present model. In contrast, the model of KF and FML had predicted the presence of a Lifshitz point at a value  $\lambda = \lambda_L$  where the phase transition crosses over from a binary liquid type transition for  $\lambda > \lambda_L$  to a microphase separation transition for  $\lambda < \lambda_L$ . However, this would not affect the predictions of the present analysis, because we are focusing on the effect of dynamical assymetries on the renormalization of the viscosity far from the transition point. As mentioned earlier, the upper critical dimension for this type of renormalization is 2, and there are no infrared divergences in three dimensions. Therefore, the viscosity renormalization remains finite in the vicinity of the phase transition.

### III. RENORMALIZED TRANSPORT COEFFICIENTS

The renormalization of the viscosity due to the dependence of the bare viscosity on the local concentration in the random copolymer melt is determined here. The method used is different from that for the renormalization due to the convective nonlinearity near a phase transition,<sup>18,19,20</sup> because the nonlinearity in the present case is dissipative. In particular, the renormalization is due to nonlinear terms in the transport equation as well as in the noise correlations, and the nonlinearities in the noise correlation are essential to ensure that the stationarity condition and the fluctuation–dissipation theorem are satisfied. Therefore, the formulation is discussed in some detail in the present analysis, and it is shown explicitly that the fluctuation–dissipation theorem is satisfied for the noise correlations used here.

The binary fluid is described by transport equations for the concentration field  $\psi$  and the velocity field  $v_\alpha$ . The Hamiltonian for the system is assumed to be of the form

$$H = \frac{1}{2} \int_{\mathbf{k}} [\psi(-\mathbf{k}, t) \chi(\mathbf{k})^{-1} \psi(\mathbf{k}, t) + \chi_v^{-1} v_\alpha(-\mathbf{k}, t) v_\alpha(\mathbf{k}, t)], \quad (13)$$

where  $\chi_v = \rho^{-1}$  is the susceptibility for the velocity field,  $\int_{\mathbf{k}}$  represents  $(2\pi)^{-3} \int d\mathbf{k}$  and Greek subscripts are used for the velocity and the wave vector. The transport equation for the concentration field is similar to that used in the Model H system of equations. As mentioned in Sec. I, we consider only the dissipative nonlinearity in the present analysis, and

neglect the nonlinearity due to the convective terms. In this case, the concentration equation is a linear equation

$$\partial_t \psi(\mathbf{k}, t) = -\Lambda_0 k_\alpha^2 \frac{\delta H}{\delta \psi(-\mathbf{k}, t)} + \theta(\mathbf{k}, t), \quad (14)$$

where  $\Lambda_0$  is the Onsager transport coefficient. The first term on the right side of the above equation represents the concentration diffusion, and the second term is the random noise which has a Gaussian distribution with zero mean and the following variance to satisfy the fluctuation–dissipation theorem:

$$\langle \theta(\mathbf{k}, t) \theta(\mathbf{k}', t') \rangle = 2k^2 \Lambda_0 \delta(\mathbf{k} + \mathbf{k}') \delta(t - t'). \quad (15)$$

The equation for the velocity field is different from that used earlier in the Model H equations due to the presence of dissipative nonlinearities, and it is useful to examine the derivation of this equation in greater detail. The microscopic equation for the velocity field is assumed to be of the form

$$\begin{aligned} \partial_t v_\alpha(\mathbf{k}, t) = & T_{\alpha\beta}(\mathbf{k}) \left[ k_\gamma \int_{\mathbf{k}'} \eta[\{\psi\}, \mathbf{k} + \mathbf{k}'] \right. \\ & \left. \times (k'_\beta v_\gamma(-\mathbf{k}', t) + \mathbf{k}'_\gamma v_\beta(-\mathbf{k}', t)) \right]. \end{aligned} \quad (16)$$

The transverse projection operator  $T_{\alpha\beta}(\mathbf{k}) = (\delta_{\alpha\beta} - \hat{k}_\alpha \hat{k}_\beta)$  ensures that the velocity field  $v_\alpha(\mathbf{k})$  is incompressible. The term on the right is the divergence of the shear stress, and in this we have assumed that the bare viscosity  $\eta$  is a function of the local concentration  $\psi(\mathbf{x}, t)$ . This term models the dynamical asymmetry in the system, where regions with different concentrations have different viscosities. In order to derive the Langevin equation, it is necessary to obtain the Fokker–Planck equation for the probability distribution  $P[\psi, v_\alpha]$  which is consistent with the microscopic equations for the concentration and velocity fields. The concentration field does not have any dissipative nonlinearities, and the Langevin equation for this is given by Eq. (14). Here, we concentrate Fokker–Planck equation for the probability distribution  $P[v_\alpha]$  of the velocity fluctuations, which is  $\int D\psi P[\psi, v_\alpha]$ . The Fokker–Planck equation consistent with the microscopic equation (16) is

$$\begin{aligned} \frac{\partial P}{\partial t} = & \int_{\mathbf{k}} \int_{\mathbf{k}'} \frac{\delta}{\delta v_\alpha(-\mathbf{k})} \left[ D_{\alpha\beta}(\psi, \mathbf{k}, \mathbf{k}') \right. \\ & \left. \times \left( \frac{\delta P}{\delta v_\beta(\mathbf{k}')} + P \frac{\delta H}{\delta v_\beta(\mathbf{k}')} \right) \right]. \end{aligned} \quad (17)$$

Note that there is no streaming velocity in the above equation because the convective nonlinearity has been neglected. The diffusion coefficient  $D_{\alpha\beta}(\psi, \mathbf{k}, \mathbf{k}')$  is

$$\begin{aligned} D_{\alpha\beta}(\psi, \mathbf{k}, \mathbf{k}') = & -T_{\alpha\gamma}(\mathbf{k}) \eta[\{\psi\}, \mathbf{k} + \mathbf{k}'] \\ & \times (k_\beta k'_\gamma + \delta_{\beta\gamma} k_\theta k'_\theta). \end{aligned} \quad (18)$$

The dependence of the diffusion coefficient on the concentration  $\psi$  causes some ambiguity in determining equivalent Langevin equation due to the following reason. The random noise is a delta function in time, and so the concentration

field  $\psi$  is a step function. Since the noise correlation is proportional to the diffusion coefficient  $D_{\alpha\beta}$ , there is some uncertainty as to whether the value of  $\psi$  to be inserted into  $D_{\alpha\beta}$  is before or after the step change; this is called the Ito–Stratonovich dilemma.<sup>21,22</sup> In the Ito formulation, the value of  $\psi$  before the step change is used, while in the Stratonovich formulation the average of the initial and final values of  $\psi$  is chosen. Different results are obtained for the correlation and response functions depending on the choice of the noise correlation. If the noise correlation is incorrectly chosen, the fluctuation–dissipation theorem may not be satisfied, and the Langevin equation written in the classical fashion may not satisfy the stationarity condition, which requires that the values of the concentration and velocity fluctuations relax to zero in the absence of the noise. This issue is considered in the Appendix, and it is shown that the Ito formulation, when coupled with the causal discretization scheme in the functional integral formalism, satisfies the stationarity condition and the fluctuation–dissipation theorem. The causal discretization scheme is convenient because the Jacobian is independent of the variables  $\psi$  and  $v_\alpha$ , and so this is used in combination with the Ito formulation in the present case as well.

In the Ito formulation, the following Langevin equation is equivalent to Eq. (17):

$$\begin{aligned} \partial_t v_\alpha(\mathbf{k}, t) = & T_{\alpha\beta}(\mathbf{k}) \left[ k_\gamma \int_{\mathbf{k}'} \eta[\{\psi\}, \mathbf{k} + \mathbf{k}'] (k'_\beta v_\gamma(-\mathbf{k}', t) \right. \\ & \left. + k'_\gamma v_\beta(-\mathbf{k}', t)) \right] + \xi_\alpha(\mathbf{k}, t). \end{aligned} \quad (19)$$

The random noise  $\xi_\alpha$  is assumed to be Gaussian white noise with zero mean and the following correlation to satisfy the fluctuation–dissipation theorem:

$$\begin{aligned} \langle \xi_\alpha(\mathbf{k}, t) \xi_\beta(\mathbf{k}', t') \rangle = & -2\chi_v \delta(t - t') T_{\alpha\xi}(\mathbf{k}) T_{\beta\eta}(\mathbf{k}') \\ & \times (k_\eta k'_\xi + \delta_{\eta\xi} k_\theta k'_\theta) \eta[\{\psi\}, \mathbf{k} + \mathbf{k}']. \end{aligned} \quad (20)$$

Note that the noise correlation is a function of the variable  $\psi$  itself, unlike in conventional mode coupling analyses where the noise correlation is a constant. Further, there are additional nonlinear terms due to the dependence of the noise on the variable  $\psi$  which have to be taken into account while determining the renormalized transport coefficients. It is shown in the Appendix that these additional nonlinearities are necessary to ensure that the fluctuation–dissipation theorem is satisfied. This will briefly be discussed when the viscosity renormalizations are calculated, and it will be shown that the fluctuation–dissipation theorem is satisfied for the present case as well.

The concentration dependent viscosity is expressed as a Taylor series in the concentration field

$$\begin{aligned} \eta[\{\psi\}, \mathbf{k} + \mathbf{k}'] = & \eta_0 \delta(\mathbf{k} + \mathbf{k}') + \eta_1 \\ & \times \int_{\mathbf{k}_1} \delta(\mathbf{k} + \mathbf{k}' + \mathbf{k}_1) \psi(-\mathbf{k}_1, t). \end{aligned} \quad (21)$$

The first term on the right is the dynamical viscosity which is independent of the concentration, while the second term on the right side takes into account the concentration dependence of the viscosity.

It is convenient to use the temporal Fourier transform of the variables  $\psi$  and  $v_\alpha$  for the functional integral formalism

$$\psi(\mathbf{q}) = \int_{-\infty}^{\infty} dt \exp(i\omega t) \psi(\mathbf{k}, t),$$

$$v_\alpha(\mathbf{q}) = \int_{-\infty}^{\infty} dt \exp(i\omega t) v_\alpha(\mathbf{k}, t),$$
(22)

where  $\mathbf{q} \equiv (\mathbf{k}, \omega)$ . The generating functional for the Langevin equation is defined as

$$\mathcal{Z} = c \int D[\psi] D[\hat{\psi}] D[v_\alpha] D[\hat{v}_\alpha] \exp(-\mathcal{L}_\psi - \mathcal{L}_v),$$
(23)

where  $c$  is the normalization constant which is independent of  $\psi$  and  $v_\alpha$  in the causal discretization, and the Lagrangians  $\mathcal{L}_\psi$  and  $\mathcal{L}_v$  are

$$\mathcal{L}_\psi = \int_{\mathbf{q}} \hat{\psi}(-\mathbf{q}) \{ [-i\omega + \Lambda_0 \chi(\mathbf{k})^{-1} k_\alpha^2] \psi(\mathbf{q}) - \theta(\mathbf{q}) \},$$

$$\mathcal{L}_v = \int_{\mathbf{q}} \hat{v}_\alpha(-\mathbf{q}) \left\{ T_{\alpha\beta}(\mathbf{k}) [-i\omega + \eta_0 k_\gamma^2] v_\beta(\mathbf{q}) - \xi_\beta(\mathbf{q}) \right. \\ \left. - \eta_1 k_\gamma \int_{\mathbf{q}_1} \int_{\mathbf{q}_2} \psi(-\mathbf{q}_2) (k_{1\gamma} v_{\beta}(-\mathbf{q}_1) + k_{1\beta} v_\gamma(-\mathbf{q}_1)) \delta(\mathbf{q} + \mathbf{q}_1 + \mathbf{q}_2) \right\}.$$
(24)

In the above equations,  $\mathcal{L}_\psi$  is obtained from Eq. (14), while  $\mathcal{L}_v$  is obtained by inserting Eq. (21) into Eq. (19). The hatted fields  $\hat{\psi}(\mathbf{q})$  and  $\hat{v}_\alpha(\mathbf{q})$  are auxiliary fields which are introduced while deriving the MSR generating functional for the Langevin equations.<sup>25</sup> These hatted fields are also related to the response functions, which give the response of the fields  $\psi$  and  $v_\alpha$  due to a perturbation in the equations of motion.

The Gaussian nature of the random noise  $\theta$  and  $\xi_\alpha$  can be used to average the Lagrangian over the distribution of the random noise. The noise averaged Lagrangian  $L_\psi = \langle \mathcal{L}_\psi \rangle$  is given by

$$L_\psi = \frac{1}{2} \int_{\mathbf{q}} [\hat{\psi}(-\mathbf{q}) \psi(-\mathbf{q})] [\mathcal{F}_{\psi\psi}^{(0)}(\mathbf{q})]^{-1} \begin{bmatrix} \hat{\psi}(\mathbf{q}) \\ \psi(\mathbf{q}) \end{bmatrix},$$
(25)

where

$$\mathcal{F}_{\psi\psi}^{(0)}(\mathbf{q})^{-1} = \begin{bmatrix} -2\Lambda_0 k_\alpha^2 & -i\omega + \Lambda_0 k_\alpha^2 \chi(\mathbf{k})^{-1} \\ i\omega + \Lambda_0 k_\alpha^2 \chi(\mathbf{k})^{-1} & 0 \end{bmatrix}.$$
(26)

The noise averaged Lagrangian  $L_v = \langle \mathcal{L}_v \rangle$  is separated into two contributions. The first  $L_v^{(0)}$ , which is due to the linear terms in the momentum equation, is similar to Eq. (26).

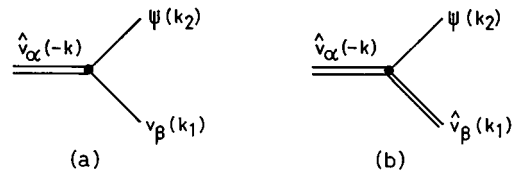


FIG. 1. Vertex functions for the determination of the renormalization in the viscosity. (a) Vertex due to nonlinearity in the transport equation. (b) Noise vertex.

$$L_v^{(0)} = \frac{1}{2} \int_{\mathbf{q}} [\hat{v}_\alpha(-\mathbf{q}) v_\alpha(-\mathbf{q})] [\mathcal{F}_{v v}^{(0)}(\mathbf{q})]^{-1} \begin{bmatrix} \hat{v}_\beta(\mathbf{q}) \\ v_\beta(\mathbf{q}) \end{bmatrix},$$
(27)

where

$$\mathcal{F}_{v v}^{(0)}(\mathbf{q})^{-1} = \begin{bmatrix} -2\eta_0 k_\gamma^2 \chi_v T_{\alpha\beta}(\mathbf{k}) & -i\omega + \eta_0 k_\gamma^2 T_{\alpha\beta}(\mathbf{k}) \\ i\omega + \eta_0 k_\gamma^2 T_{\alpha\beta}(\mathbf{k}) & 0 \end{bmatrix}.$$
(28)

For future reference, the correlation and response functions in the linear approximation, which can be easily calculated from the above Lagrangians, are

$$\hat{G}_{\psi\psi}(\mathbf{q}) = \langle \hat{\psi}(-\mathbf{q}) \psi(\mathbf{q}) \rangle, \\ = \frac{1}{-i\omega + \Lambda_0 k_\alpha^2 \chi(\mathbf{k})^{-1}},$$
(29)

$$G_{\psi\psi}(\mathbf{q}) = \langle \psi(-\mathbf{q}) \psi(\mathbf{q}) \rangle, \\ = \chi(\mathbf{k}) \left[ \frac{1}{-i\omega + \Lambda_0 k_\alpha^2 \chi(\mathbf{k})^{-1}} + \frac{1}{i\omega + \Lambda_0 k_\alpha^2 \chi(\mathbf{k})^{-1}} \right],$$

$$\hat{G}_{v_\alpha v_\beta}(\mathbf{q}) = \langle \hat{v}_\beta(-\mathbf{q}) v_\alpha(\mathbf{q}) \rangle, \\ = \frac{T_{\alpha\beta}(\mathbf{k})}{-i\omega + \eta_0 k_\alpha^2},$$

$$G_{v_\alpha v_\beta} = \langle v_\beta(-\mathbf{q}) v_\alpha(\mathbf{q}) \rangle, \\ = \chi_v T_{\alpha\beta}(\mathbf{k}) \left[ \frac{1}{-i\omega + \eta_0 k_\gamma^2} + \frac{1}{i\omega + \eta_0 k_\gamma^2} \right].$$
(30)

The second contribution  $L_v^{(1)}$ , due to the nonlinear terms in the transport equation and  $\psi$  dependent terms in the noise correlation, is

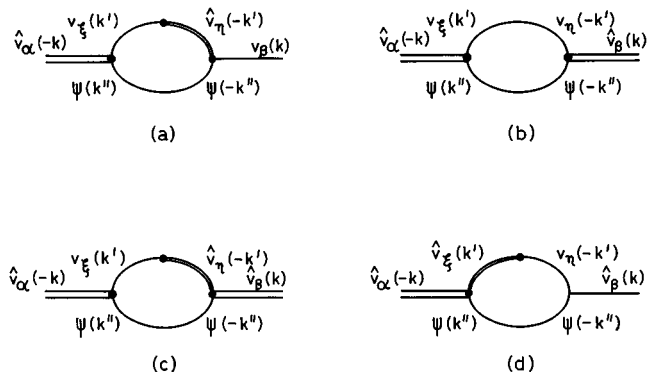


FIG. 2. One loop expansions for the correlation function (a) and response function (b), (c), and (d) for the correlation function.

$$L_v^{(1)} = \int_{\mathbf{q}} \int_{\mathbf{q}'} \hat{v}_\alpha(-\mathbf{q}) [-F_{\alpha\beta}(\{\psi\}, \mathbf{q}, \mathbf{q}') v_\beta(-\mathbf{q}') + 2F_{\alpha\beta}(\{\psi\}, \mathbf{q}, \mathbf{q}') \hat{v}_\beta(-\mathbf{q}')], \quad (31)$$

where

$$F_{\alpha\beta}(\{\psi\}, \mathbf{q}, \mathbf{q}') = T_{\alpha\xi}(\mathbf{k}) T_{\beta\eta}(\mathbf{k}') (k_\eta k'_\xi + \delta_{\eta\xi} k_\theta k'_\theta) \times \left[ \eta_1 \int_{\mathbf{q}_1} \psi(-\mathbf{q}_1) \delta(\mathbf{q} + \mathbf{q}' + \mathbf{q}_1) \right]. \quad (32)$$

In Eq. (31), the first term on the right side represents the nonlinear terms in the transport equations (19), while the

second term is due to the  $\psi$  dependent terms in the noise correlation (20). Each of these gives rise to a three point vertex as shown in Fig. 1.

In the renormalized perturbation expansion, the effect of the nonlinear terms is expressed as the self-energy for the correlation and response functions,  $\Sigma_{vv}$  and  $\hat{\Sigma}_{vv}$ , and the renormalized Lagrangian for the velocity correlations  $L_v$  is

$$L_v = \frac{1}{2} \int_{\mathbf{q}} [\hat{v}_\alpha(-\mathbf{q}) v_\alpha(-\mathbf{q})] [\mathcal{S}_{vv}(\mathbf{q})^{-1}] \begin{bmatrix} \hat{v}_\beta(\mathbf{q}) \\ v_\beta(\mathbf{q}) \end{bmatrix}, \quad (33)$$

where

$$\mathcal{S}_{vv}(\mathbf{q})^{-1} = \begin{bmatrix} (-2\eta_0 k_\gamma^2 \chi_v - \Sigma_{vv}(\mathbf{q})) T_{\alpha\beta}(\mathbf{k}) & (-i\omega + \eta_0 k_\gamma^2 - \hat{\Sigma}_{vv}(\mathbf{q})) T_{\alpha\beta}(\mathbf{k}) \\ (i\omega + \eta_0 k_\gamma^2 - \hat{\Sigma}_{vv}(-\mathbf{q})) T_{\alpha\beta}(\mathbf{k}) & 0 \end{bmatrix}. \quad (34)$$

It is shown in the Appendix that with the above choice of the noise correlations (20) and (21), the self-energies  $\Sigma_{vv}$  and  $\hat{\Sigma}_{vv}$  satisfy the Onsager reciprocal relations and the fluctuation dissipation theorem to all orders in the perturbation theory, and therefore the renormalized viscosity has the same value whether it is determined using  $\Sigma_{vv}$  or  $\hat{\Sigma}_{vv}$ . The renormalized viscosity determined from the response and correlation functions is

$$\eta_R - \eta_0 = \lim_{\mathbf{q} \rightarrow 0} k_\alpha^{-2} (-\hat{\Sigma}_{vv}) = (1/2) \chi_v^{-1} \lim_{\mathbf{q} \rightarrow 0} k_\alpha^{-2} \Sigma_{vv}. \quad (35)$$

In the following analysis, we verify that the two renormalizations are equal, and therefore the fluctuation-dissipation theorem is satisfied.

The leading order contribution to the self-energy  $\hat{\Sigma}_{vv}^{(1)}$  due to the  $O(\psi)$  correction to the viscosity is due to the one-loop diagram shown in Fig. 2(a)

$$\hat{\Sigma}_{vv}^{(1)} = \eta_1^2 \int_{\mathbf{q}} (k_\xi k'_\alpha + \delta_{\alpha\xi} k_\gamma k'_\gamma) (k_\eta k'_\beta + \delta_{\beta\eta} k_\theta k'_\theta) \times T_{\alpha\beta}(\mathbf{k}) T_{\xi\eta}(\mathbf{k}') G_{\psi\psi}(\mathbf{q} - \mathbf{q}') \hat{G}_{vv}(\mathbf{q}'). \quad (36)$$

The leading order contribution to  $\Sigma_{vv}^{(1)}$  due to the  $O(\psi)$  correction to the viscosity is given by the three diagrams shown in Figs. 2(b), 2(c), and 2(d). The first diagram is due to the nonlinearity in the transport equation (19) and (21), while the last two are due to the nonlinearities in the noise correlations in Eqs. (20) and (21) (the presence of two diagrams is because there is a degeneracy due to the presence of nonidentical vertices). The contribution to the self-energies can be simplified using

$$G_{v_\alpha v_\beta}(\mathbf{q}) = \chi_v (\hat{G}_{v_\alpha v_\beta}(\mathbf{q}) + \hat{G}_{v_\alpha v_\beta}(-\mathbf{q})) \quad (37)$$

from Eq. (30). Using this, it can easily be verified that the diagram in Fig. 2(b) is the negative of half the sum of the diagrams in Figs. 2(c) and 2(d), and the total contribution to  $\Sigma_{vv}$  is just half the sum of the last two diagrams

$$\Sigma_{vv}^{(1)} = -\eta_1^2 \int_{\mathbf{q}} (k_\xi k'_\alpha + \delta_{\alpha\xi} k_\gamma k'_\gamma) (k_\eta k'_\beta + \delta_{\beta\eta} k_\theta k'_\theta) \times T_{\alpha\beta}(\mathbf{k}) T_{\xi\eta}(\mathbf{k}') G_{\psi\psi}(\mathbf{q} - \mathbf{q}') G_{vv}(\mathbf{q}'). \quad (38)$$

From Eq. (30) for the correlation and response functions, it can be easily verified that Eqs. (36) and (38) give identical corrections for the viscosity renormalization in the long time limit  $\omega \rightarrow 0$ , and the formulation of the first order corrections is consistent with the fluctuation-dissipation theorem.

Equation (36) for  $\hat{\Sigma}_{vv}^{(1)}$  can be simplified in the limit  $\omega \rightarrow 0$  to obtain

$$\hat{\Sigma}_{vv}^{(1)}(\mathbf{k}) = \frac{\eta_1^2 k^2}{5\pi^2} \int dk' k'^2 \frac{k'^2 \chi(\mathbf{k}'')}{\lambda \chi(\mathbf{k}'')^{-1} k''^2 + \eta_0 k'^2}. \quad (39)$$

In the liquid state, where the viscous relaxation is much faster than the molecular diffusion, the first term in denominator of the above integrand can be neglected compared to the second term, and in the limit  $k \rightarrow 0$  we get

$$\hat{\Sigma}_{vv}^{(1)} = \frac{\eta_1^2 k^2}{5\pi^2 \eta_0} \int dk' k'^2 \chi(\mathbf{k}'). \quad (40)$$

Using Eq. (40), the renormalized viscosity due to the dynamical asymmetry can be written as

$$\eta_R - \eta_0 = -\frac{\eta_1^2}{5\pi^2 \eta_0} \int_{\mathbf{k}'} k'^2 \chi(\mathbf{k}'). \quad (41)$$

The above equation, together with Eqs. (11) and (12) for the structure factor, gives the variation in the viscosity due to the correlations in the sequence distribution in the random copolymer. It is useful to discuss two important issues regarding the renormalization (41) at this stage.

(1) The integral over the wave vector does not have any infrared ( $k \rightarrow 0$ ) divergences above two dimensions, so the upper critical dimension for the viscosity renormalization is 2. This is in contrast to the renormalization due to convective nonlinearities, where the upper critical dimension is 4 and

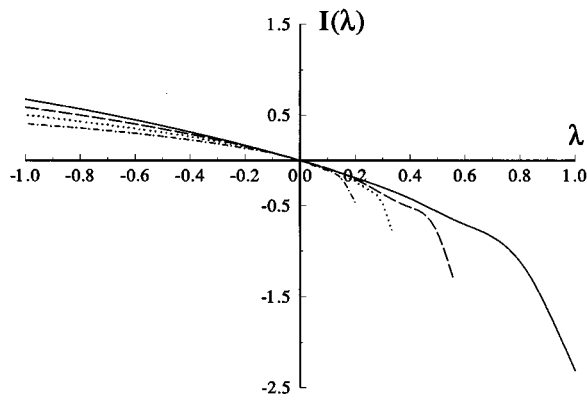


FIG. 3.  $I(\lambda)$  as a function of  $\lambda$  for different values of  $\kappa=f(1-f)\chi_F$ . (—)  $\kappa=0$ ; (---)  $\kappa=0.2$ ; (···)  $\kappa=0.5$ ; (-.-)  $\kappa=1.0$ .

there are divergences in the transport coefficients in three dimensions. Therefore, the present renormalization is convergent as the critical point is approached, and could be important even far from the critical point. In addition, there are no ultraviolet divergences because the self-component of the structure factor has been removed while determining the equations for the structure factor (11) and (12).

(2) It is important to emphasize that the viscosity correction is proportional to  $\eta_1^2$ , and so it is independent of the sign of  $\eta_1$  and depends only on the monomer sequence distribution. In other words, the renormalization is not influenced by whether the viscosity is higher for regions with positive  $\psi$  (rich in monomer  $A$ ) or regions with negative  $\psi$  (rich in monomer  $B$ ), the correction depends only on the ordering sequence of the monomers on the chain.

The factor  $I(\lambda) = -\int dk' k'^2 \chi(\mathbf{k}')$ , which is proportional to the viscosity renormalization, is shown as a function of the parameter  $\lambda$  for different values of  $\kappa=f(1-f)\chi_F$  in Fig. 3. In this case, we have assumed that the Flory  $\chi$  parameter is local (independent of  $k$ ); it is easy to include nonlocal interactions as well. This figure shows that there is an increase in the viscosity for  $\lambda < 1$ , and a decrease in the viscosity for  $\lambda > 1$ . Figure 3 also shows the variation in the viscosity as the enthalpic repulsion  $\chi_F$  is varied. It can be seen that the magnitude of the renormalization in the viscosity decreases for  $\lambda < 0$ , and increases for  $\lambda > 0$ . The graphs for  $I(\lambda)$  terminate at specific value of  $\lambda$  for  $\chi_F > 0$  because the model used here predicts a phase transition at this point. It can be seen that the renormalization in the viscosity remains finite at this point, as anticipated earlier, because the upper critical dimension for the dissipative nonlinearity is 2.

#### IV. CONCLUSIONS

The effect of monomer sequence distribution on the dynamical viscosity of a random copolymer was considered in the present study using a simple model for a random copolymer consisting of two types of monomers,  $A$  and  $B$ . The usual Markov model was used, where the random copolymer is specified by the fraction of type  $A$  monomers  $f$ , the Flory chi parameter which gives the strength of the enthalpic repulsion and the parameter  $\lambda$  which gives the correlation in

monomer identities along the chain. The model used here is similar to that used in the previous studies of Fredrickson, Helfand, and Milner<sup>17</sup> and Kumaran and Fredrickson,<sup>18</sup> though a modification in the form of the structure factor was necessary to avoid ultraviolet divergences in the calculations. Due to this, the thermodynamics of the present model is different. There is a binary fluid type phase transition for  $\lambda > 0$  (where there is a greater probability of finding like monomers adjacent to each other on the chain), and there is no phase transition for  $\lambda < 0$  (where it is more likely that unlike monomers are adjacent on the chain). The structure factor determined in this fashion was then used in a mode coupling calculation to determine the dependence of the viscosity on the sequence distribution.

The model equations for the mode coupling calculation are similar to the Model H equations used in critical dynamics, but the momentum equation is modified to include the possibility of the dependence of viscosity on the local concentration. This type of variation could be present if the viscosities of pure  $A$  and  $B$  polymers are very different, so that the local viscosity depends on the relative ratios of monomers of type  $A$  and  $B$ . The mode coupling calculations are different in the present case; because the nonlinearity in the momentum equation is dissipative in nature. Due to this, there is some ambiguity in the interpretation of the noise correlations; this is discussed in the Appendix. Here, we have used one particular interpretation of the noise correlation which is consistent with the causal discretization method used in the functional integral formalism, and it has also been explicitly verified that the present formulation is consistent and the fluctuation-dissipation theorem is satisfied. Another difference between the present calculation and earlier critical dynamics studies is that the upper critical dimension for the present case is 2, in contrast to the UCD of 4 in critical dynamics. Therefore, the renormalization in the viscosity remains finite in the vicinity of a phase transition.

The results indicate that there is a systematic variation in the viscosity with the parameter  $\lambda$ , and the fluctuations tend to increase the viscosity for  $\lambda < 0$  and decrease the viscosity for  $\lambda > 0$ . Further, the sign of the renormalization does not depend on whether an increase in the concentration of  $A$  monomers increases or decreases the viscosity, but on the parameter  $\lambda$  alone, because the renormalization in the viscosity is proportional to  $\eta_1^2$ , where  $\eta_1$  is the variation in the viscosity with concentration. This indicates that the renormalization in the viscosity is purely due to differences in the correlation in the monomer identities along the chain. The present renormalization could be important even far from a phase transition, since the magnitude does not depend on the difference between the temperature and the transition temperature. In addition, this could be the dominant effect even near a phase transition of the binary fluid type, because the earlier critical dynamics study of KF showed that the renormalization due to convective effects has a very small divergence near a binary fluid type transition. Though the model used here is rather crude, some very definite variations in the viscosity as a function of the correlation in the monomer identities and the temperature are predicted, and we feel that

the present study captures qualitatively the essential dynamics of random copolymers. This could provide a useful starting point for more detailed analyses, where the microscopic dynamics of the polymer are taken into account, and could also motivate experiments on the viscosity measurements on random copolymers synthesized under controlled conditions.

## ACKNOWLEDGMENT

The author would like to thank Professor G. H. Fredrickson for useful discussions.

## APPENDIX

In this Appendix, a functional integral formalism is used to show that the Ito formulation for the nonlinear Langevin equation, with the noise correlation given by the Ito prescription, when coupled with a causal discretization scheme, satisfies the stationarity condition, the fluctuation–dissipation theorem and the Onsager reciprocal relations. Consider a general Fokker–Planck equation for a system described by time dependent variables  $\psi_i(\mathbf{k}, t)$

$$\partial_t P = \int_{\mathbf{k}} \int_{\mathbf{k}'} \frac{\delta}{\delta \psi(-\mathbf{k}, t)} \left[ \Gamma_{ij}(\{\psi\}, \mathbf{k}, \mathbf{k}') \times \left( \frac{\delta H}{\delta \psi_j(\mathbf{k}', t)} P + \frac{\delta P}{\delta \psi_j(\mathbf{k}', t)} \right) \right], \quad (\text{A1})$$

where the Hamiltonian is given by

$$H(\{\psi\}) = \sum_i \int d\mathbf{k} \psi_i(-\mathbf{k}) \chi_i(\mathbf{k})^{-1} \psi_i(\mathbf{k}). \quad (\text{A2})$$

Note that the above form of the Hamiltonian is quite general, and even if the Hamiltonian contains terms of the type  $\psi_i(-\mathbf{k}) \chi_{ij}(\mathbf{k})^{-1} \psi_j(\mathbf{k})$ , it can be reduced to the above form by diagonalizing the matrix  $\chi_{ij}(\mathbf{k})$ . In Eq. (A1), we have explicitly included the  $\{\psi\}$  dependence of the transport coefficients, and neglected the convective (streaming) term for notational simplicity. In the Ito formulation, the nonlinear Langevin equation is

$$\partial_t \psi_i(\mathbf{k}, t) = \int_{\mathbf{k}'} \sum_j \left[ -\Gamma_{ij}(\{\psi\}, \mathbf{k}, \mathbf{k}') \frac{\delta H}{\delta \psi_j(\mathbf{k}', t)} + \frac{\delta [\Gamma_{ij}(\{\psi\}, \mathbf{k}, \mathbf{k}')]}{\delta \psi_j(\mathbf{k}', t)} \right] + C_i(\{\psi\}, \mathbf{k}) \theta(t). \quad (\text{A3})$$

The transport coefficients  $\Gamma_{ij}$  are real because they represent dissipative effects, and are constrained by the Onsager reciprocal relations

$$\Gamma_{ij}(\{\psi\}, \mathbf{k}, \mathbf{k}') = \Gamma_{ji}(\{\psi\}, \mathbf{k}', \mathbf{k}). \quad (\text{A4})$$

Note that the transport coefficient is now dependent on the time  $t$ , even though we have neglected memory effects, due to the variation of  $\{\psi\}$  in time. The nonlinear Langevin equation (A3) differs from the linear Langevin equation due to the presence of the term  $(\delta \Gamma_{ij} / \delta \psi_j)$ . In Eq. (A3), the noise has been written as a product of two components. The coef-

ficients  $C_i$  depend on the values of the variables  $\{\psi\}$ , but do not depend explicitly on time. These are related to the transport coefficients

$$C_i(\{\psi\}, \mathbf{k}) C_j(\{\psi\}, \mathbf{k}') = \Gamma_{ij}(\{\psi\}, \mathbf{k}, \mathbf{k}') + \Gamma_{ji}(\{\psi\}, \mathbf{k}', \mathbf{k}). \quad (\text{A5})$$

The term  $\theta$  represents the rapidly fluctuating component of the noise which has the following averages:

$$\langle \theta(t) \rangle = 0, \quad (\text{A6})$$

$$\langle \theta(t) \theta(t') \rangle = \delta(t - t'). \quad (\text{A7})$$

In addition, for the Langevin equation (A3) to mimic the FP equation (A1), it is necessary to take the values of  $\{\psi\}$  at the beginning of the time interval while evaluating  $C_i$ . The discretized form of the Langevin equation (A3) is given by

$$\frac{\psi_i(t + \Delta t) - \psi_i(t)}{\Delta t} = \int_{\mathbf{k}'} \sum_j \left[ -\Gamma_{ij}(\{\psi(t)\}, \mathbf{k}, \mathbf{k}') \frac{\delta H}{\delta \psi_j(\mathbf{k}', t)} + \frac{\delta \Gamma_{ij}(\{\psi(t)\}, \mathbf{k}, \mathbf{k}')}{\delta \psi_j(\mathbf{k}', t)} \right] + C_i(\{\psi(t)\}, \mathbf{k}) \times \frac{1}{\Delta t} \int_t^{t+\Delta t} dt' \theta(t'). \quad (\text{A8})$$

The set of nonlinear Langevin equations (A3) with the definition of the noise given by Eqs. (A5), (A6), and (A7) have been shown to be formally equivalent to the nonlinear FP equation (A1) by Ito.<sup>21</sup> Moreover, the FP equation satisfies the stationarity condition and the fluctuation dissipation theorem, and we would expect the Langevin equation to satisfy these conditions as well. In this Appendix, we show analytically, independently of the FP equation, that Eq. (A3) satisfies these conditions at all orders in perturbation theory. For this purpose, a functional integral formalism is used, and the renormalization due to the nonlinear terms in the Langevin equations are determined using a diagrammatic perturbation theory. Various discretization schemes have been used in the functional integral approach.<sup>25–27</sup> Of these, the causal discretization scheme of Jensen<sup>25</sup> is suitable for the present formulation, since it gives the same interpretation of the noise correlations as the Ito prescription (A8). In addition, this scheme has the advantage that the Jacobian in the generating functional is independent of the variables  $\{\psi\}$ , while in the other schemes, the Jacobian is explicitly dependent on  $\{\psi\}$  and the calculations are more complicated (see Jensen<sup>25</sup> for a detailed discussion).

For the functional integral formalism, it is convenient to take the temporal Fourier transforms of the variables  $\psi_i$

$$\psi_i(\mathbf{q}) = \int dt \exp(i\omega t) \psi_i(\mathbf{k}, t), \quad (\text{A9})$$

where  $\mathbf{q} = (\mathbf{k}, \omega)$ . A generating functional  $\mathcal{Z}$  for the Langevin equation (A3) is defined as follows:

$$\begin{aligned} \mathcal{Z} = & \int \prod_i D[\psi_i] J[\psi_i] \delta\left(-i\omega\psi_i(\mathbf{q}) + \Gamma_{ij}(\{\psi\}, \mathbf{k}, \mathbf{k}') \right. \\ & \left. \times \frac{\delta H}{\delta\psi_j(\mathbf{q}')} - \frac{\delta\Gamma_{ij}(\{\psi\}, \mathbf{k}, \mathbf{k}')}{\delta\psi_j(\mathbf{q}')} - C_i(\{\psi\}, \mathbf{k})\theta(\omega)\right), \end{aligned} \quad (\text{A10})$$

where  $J[\psi_i]$  is a Jacobian associated with the delta function, and enforces the normalization condition  $\mathcal{Z}=1$ . In the causal discretization scheme, the Jacobian turns out to be independent of  $\{\psi\}$ , and this simplifies the calculation. The delta function in Eq. (A10) is transformed into its functional Fourier transform

$$\mathcal{Z} = c \int \prod_i D[\psi_i] D[\hat{\psi}_i] \exp(-\mathcal{L}), \quad (\text{A11})$$

where the factor  $c$  contains the Jacobians that are independent of  $\{\psi\}$ , and the Lagrangian  $\mathcal{L}$  is

$$\begin{aligned} \mathcal{L} = & \int_{\mathbf{q}} \hat{\psi}_i(-\mathbf{q}) \left[ -i\omega\psi_i(\mathbf{q}) + \int_{\mathbf{q}'} \left( \Gamma_{ij}(\{\psi\}, \mathbf{k}, \mathbf{k}') \chi_j^{-1}(\mathbf{k}') \right. \right. \\ & \left. \left. \times \psi_j(-\mathbf{q}') - \frac{\delta\Gamma_{ij}(\{\psi\}, \mathbf{k}, \mathbf{k}')}{\delta\psi_j(\mathbf{q}')} \right) - C_i(\{\psi\}, \mathbf{k})\theta(\omega) \right], \end{aligned} \quad (\text{A12})$$

where  $\int_{\mathbf{q}}$  is  $(2\pi)^{-4} \int d\mathbf{k} \int d\omega$ . The Gaussian nature of the random noise can be effectively utilized to explicitly average the Lagrangian over the noise distribution. The noise averaged generating functional is

$$Z = \langle \mathcal{Z} \rangle = c \int \prod_i D[\psi_i] D[\hat{\psi}_i] \exp(-L), \quad (\text{A13})$$

where

$$\begin{aligned} L = & \int_{\mathbf{q}} \hat{\psi}_i(-\mathbf{q}) \left[ -i\omega\psi_i(\mathbf{q}) + \int_{\mathbf{q}'} \left( \Gamma_{ij}(\{\psi\}, \mathbf{k}, \mathbf{k}') \chi_j^{-1}(\mathbf{k}') \right. \right. \\ & \left. \left. \times \psi_j(-\mathbf{q}') - \frac{\delta\Gamma_{ij}(\{\psi\}, \mathbf{k}, \mathbf{k}')}{\delta\psi_j(\mathbf{q}')} + [\Gamma_{ij}(\{\psi\}, \mathbf{k}, \mathbf{k}')] \right. \right. \\ & \left. \left. + \Gamma_{ji}(\{\psi\}, \mathbf{k}', \mathbf{k}) \hat{\psi}_j(-\mathbf{q}') \right) \right]. \end{aligned} \quad (\text{A14})$$

Equation (A13) for the generating functional with the Lagrangian given by Eq. (A14) serves as a starting point for the perturbation analysis.

The transport coefficient is expanded in a Taylor series in the  $\{\psi\}$  as follows:

$$\begin{aligned} \Gamma_{ij}(\{\psi\}, \mathbf{k}, \mathbf{k}') = & \Gamma_{ij}^{(0)}(\mathbf{k}) \delta(\mathbf{k} + \mathbf{k}') + \sum_m \int_{\mathbf{q}_1} \Gamma_{ijm}^{(1)}(\mathbf{k}, \mathbf{k}', \mathbf{k}_1) \\ & \times \psi_m(-\mathbf{q}_1) \delta(\mathbf{q} + \mathbf{q}' + \mathbf{q}_1) \\ & + \sum_{m,n} \int_{\mathbf{q}_1} \int_{\mathbf{q}_2} \Gamma_{ijmn}^{(2)}(\mathbf{k}, \mathbf{k}', \mathbf{k}_1, \mathbf{k}_2) \psi_m(-\mathbf{q}_1) \\ & \times \psi_n(-\mathbf{q}_2) \delta(\mathbf{q} + \mathbf{q}' + \mathbf{q}_1 + \mathbf{q}_2) + \dots \end{aligned} \quad (\text{A15})$$

In Eq. (A15), the first term does not depend on time, because we have neglected memory effects, but the higher order terms depend implicitly on time due to their dependence on  $\{\psi\}$ . Equation (A15) is inserted into the equation for the Lagrangian, which is then divided into its Gaussian and perturbative components,  $L_0$  and  $L_p$ . The Gaussian component,  $L_0$ , can be written in symmetrized form as follows:

$$L_0 = \frac{1}{2} \int_{\mathbf{q}} [[\hat{\psi}(-\mathbf{q})]^T [\psi(-\mathbf{q})]^T] [G^{(0)}(\mathbf{q})]^{-1} \begin{bmatrix} \hat{\psi}(\mathbf{q}) \\ \psi(\mathbf{q}) \end{bmatrix}. \quad (\text{A16})$$

Here,  $[\hat{\psi}]$  and  $[\psi]$  are the column matrices  $[\hat{\psi}_1, \hat{\psi}_2, \dots, \hat{\psi}_N]$  and  $[\psi_1, \psi_2, \dots, \psi_N]$ , respectively, and  $G_0^{-1}$  is the block diagonal matrix consisting of three  $N \times N$  blocks

$$\begin{aligned} [G^{(0)}(\mathbf{q})]^{-1} = & \begin{bmatrix} -[\Gamma^{(0)}(\mathbf{k})] - [\Gamma^{(0)}(-\mathbf{k})]^T & [-i\omega I + \Lambda^{(0)}(\mathbf{k})] \\ [i\omega I + \Lambda^{(0)}(-\mathbf{k})]^T & 0 \end{bmatrix}, \end{aligned} \quad (\text{A17})$$

where  $I$  is the identity matrix and  $\Lambda_{ij}^{(0)}(\mathbf{k}) = \Gamma_{ij}^{(0)}(\mathbf{k}) \chi_j^{-1}(\mathbf{k})$ .

In the Gaussian approximation, the statistical average of an analytical function  $A(\{\hat{\psi}\}, \{\psi\})$  can be expressed as

$$\begin{aligned} \langle A(\{\hat{\psi}\}, \{\psi\}) \rangle_0 = & c \int \prod_i D[\hat{\psi}_i] D[\psi_i] A(\{\hat{\psi}\}, \{\psi\}) \\ & \times \exp(-L_0), \end{aligned} \quad (\text{A18})$$

where the subscript  $_0$  implies that this is the Gaussian average. Of particular interest are the correlation and response functions,  $G_{ij}^{(0)}(\mathbf{q})$  and  $\hat{G}_{ij}^{(0)}(\mathbf{q})$ , which are defined as

$$\hat{G}_{ij}^{(0)}(\mathbf{q}) = \langle \hat{\psi}_j(-\mathbf{q}) \psi_i(\mathbf{q}) \rangle_0 = [-i\omega I + \Lambda^{(0)}(\mathbf{k})]_{ij}^{-1}, \quad (\text{A19})$$

$$\begin{aligned} G_{ij}^{(0)}(\mathbf{q}) = & \langle \psi_j(-\mathbf{q}) \psi_i(\mathbf{q}) \rangle_0 \\ = & [-i\omega I + \Lambda^{(0)}(\mathbf{k})]_{il}^{-1} \\ & \times [\Gamma_{lm}^{(0)}(\mathbf{k}) + \Gamma_{ml}^{(0)}(-\mathbf{k})] [i\omega I + \Lambda^{(0)}(-\mathbf{k})]_{jm}^{-1}. \end{aligned} \quad (\text{A20})$$

It can be easily verified from Eqs. (A19) and (A20) that the correlation and response functions are related as follows:

$$\hat{G}_{ij}(\mathbf{q}) \chi_j(\mathbf{k}) = \hat{G}_{ji}(\mathbf{q}) \chi_i(\mathbf{k}), \quad (\text{A21})$$

$$G_{ij}(\mathbf{q}) = \hat{G}_{ij}(\mathbf{q}) \chi_j(\mathbf{k}) + \hat{G}_{ji}(-\mathbf{q}) \chi_i(\mathbf{k}). \quad (\text{A22})$$

The first equation (A21) is a due to the Onsager reciprocal relations, while the second equation (A22) is a consequence of the fluctuation dissipation theorem.

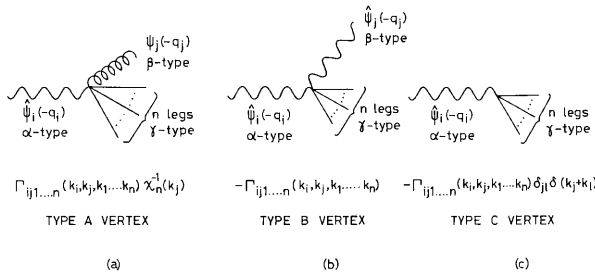


FIG. 4. Types of vertices due to nonlinear terms in the diagrammatic perturbation expansion.

There are two rules to be adhered to while computing averages in the causal discretization scheme. The first is that the averages of products containing the factors  $\hat{\psi}_i(t)$  vanish if  $t$  is the latest time in the average. In particular, an average containing two response functions is always zero

$$\langle \hat{\psi}(\mathbf{q}) \hat{\psi}(\mathbf{q}') \rangle_0 = 0. \tag{A23}$$

The second rule is that the averages of products  $\langle \hat{\psi}_i(\mathbf{k}, t) \psi_j(\mathbf{k}', t) \rangle_0$  are interpreted as if the time arguments of the hatted fields are displaced to infinitesimally later times, and therefore average to zero. In particular, the following relation will be useful in the subsequent analysis:

$$\hat{G}_{ij}(\mathbf{k}, t)|_{t=0} = \int_{-\infty}^{\infty} d\omega \hat{G}_{ij}(\mathbf{q}) = 0. \tag{A24}$$

Before proceeding to the perturbation analysis, it is useful to discuss the objective of this analysis. Our objective is to show that the Langevin equations (A3), when combined with the causal discretization scheme, give results for the first and second moments which are consistent with the requirements of stationarity, the Onsager reciprocal relations

$$[G(\mathbf{q})]^{-1} = [G^{(0)}(\mathbf{q})]^{-1} - [\Pi] = \begin{bmatrix} -[\Gamma^{(0)}(\mathbf{k})] - [\Gamma^{(0)}(-\mathbf{k})]^T - [\Sigma(\mathbf{q})] & [-i\omega I + \Lambda^{(0)}(\mathbf{k})] - [\hat{\Sigma}(\mathbf{q})] \\ [i\omega I + \Lambda^{(0)}(-\mathbf{k})]^T - [\hat{\Sigma}(-\mathbf{q})]^T & 0 \end{bmatrix}, \tag{A26}$$

where  $[\Pi]$ , the self-energy matrix, has a block diagonal form similar to  $[G^{(0)}]^{-1}$ . For the fluctuation dissipation theorem to be satisfied,<sup>28</sup> the elements of the diagonal block  $\Sigma_{ij}$  and the off-diagonal block  $\hat{\Sigma}_{ij}$  of the self-energy matrix have to be related in a manner similar to those of the matrix  $[G^{(0)}]^{-1}$  [see Eq. (A17)]

$$\Sigma_{ij}(\mathbf{q}) + \hat{\Sigma}_{ij}(\mathbf{q})\chi_j(\mathbf{k}) + \hat{\Sigma}_{ji}(-\mathbf{q})\chi_i(\mathbf{k}) = 0 \tag{A27}$$

and

$$\hat{\Sigma}_{ij}(\mathbf{q})\chi_j(\mathbf{k}) = \hat{\Sigma}_{ji}(\mathbf{q})\chi_i(\mathbf{k}). \tag{A28}$$

In the remainder of this section, we use a perturbation analy-

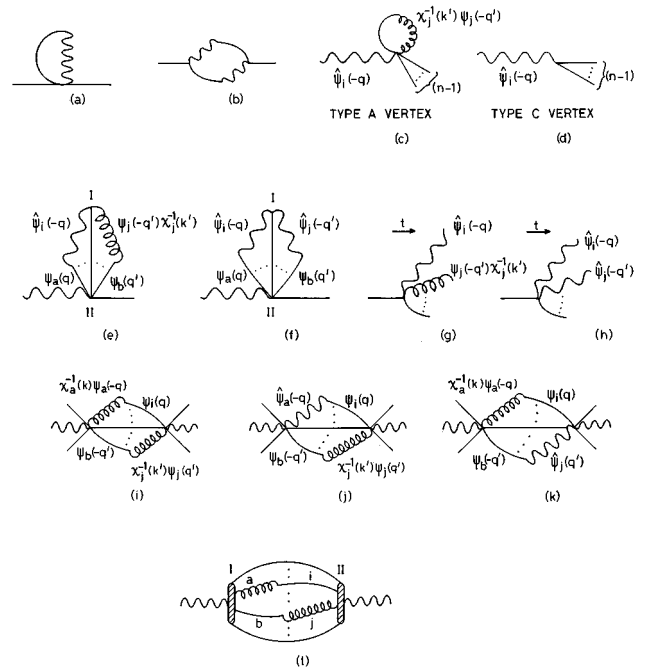


FIG. 5. Diagrammatic representations of Rules 1 to 6 in the Appendix.

sis to show that Eqs. (A25), (A27), and (A28) are satisfied by the self-energies for a Langevin equation of the type (A3) with the noise correlation given by Eqs. (A5), (A6), and (A7).

and the fluctuation–dissipation theorem. The stationarity condition requires that the average value of a variable  $\psi_i$  be equal to its equilibrium value

$$\langle \psi_i \rangle = \langle \hat{\psi}_i \rangle = 0. \tag{A25}$$

Note that the averages in the above equation are not the bare averages, but include the effect of the nonlinearities. The second consistency condition follows from the fluctuation dissipation theorem. For this, consider the coefficient matrix  $[G^{(0)}]^{-1}$  in the equation for the bare Lagrangian  $L_0$  (A17). The nonlinear terms renormalize this coefficient matrix

It is convenient to classify the nonlinear vertices into three categories. The first, called type A, is due to the nonlinearity in the transport coefficient in the Langevin equation (A3). If the transport coefficient is proportional to  $\psi''$ , this vertex has  $n+2$  legs, as shown in Fig. 4(a). The type A vertices have the following symmetries, the first due to the Onsager reciprocal relations and the second due to the invariance of the irreversible term in the transport coefficient under spatial inversion

$$\Gamma_{ij1\dots n}(\mathbf{k}, \mathbf{k}', \mathbf{k}_1, \dots, \mathbf{k}_n) = \Gamma_{ji1\dots n}(\mathbf{k}', \mathbf{k}, \mathbf{k}_1, \dots, \mathbf{k}_n), \tag{A29}$$

$$\Gamma_{ij1\dots n}(\mathbf{k}, \mathbf{k}', \mathbf{k}_1, \dots, \mathbf{k}_n) = \Gamma_{ij1\dots n}(-\mathbf{k}, -\mathbf{k}', -\mathbf{k}_1, \dots, -\mathbf{k}_n).$$

The second type of vertex, type *B*, is due to the nonlinearity in the noise correlations. This also has  $n + 2$  legs, as shown in Eq. (A3), but two of the legs are of the hatted type. The third type of vertex, type *C*, is due to the term  $(\delta\Gamma_{ij}/\delta\psi_j)$  in Eq. (A3). This vertex has  $n$  legs, one of which is the hatted type. It is also useful to classify the legs in the type *A* vertex into three categories. The hatted leg is called the  $\alpha$  leg, while the unhatted leg due to the functional derivative of the free energy [the  $j$  leg in Fig. 4(a)] is called the  $\beta$  leg and all the other legs are  $\gamma$  legs. In the type *B* vertex, the  $\alpha$  and  $\beta$  legs are both of the hatted type. In the diagrammatic perturbation analysis, it will be convenient to refer to the topological features in terms of these classifications.

At this point, it is necessary to specify certain rules which simplify the determination of the values of the diagrams. The first two are fairly simple and common to all diagrammatic perturbation expansions, but we list them here for completeness.

*Rule 1.* A graph having a bubble of the type shown in Fig. 5(a) is identically zero. This is because this bubble represents equation (A24).

*Rule 2.* A graph having a loop of the type shown in Fig. 5(b) is zero due to causality. This is also true for renormalized vertices in general, provided we adhere to the convention that time increases from left to right or vice versa.

*Rule 3.* A graph having a bubble which involves a type *A* vertex with a  $\beta$  leg [Fig. 5(c)] is exactly canceled by another graph with a type *C* vertex [Fig. 5(d)]. This can be easily seen by writing down the values of the two graphs. The value of the graph 5(c) is

$$\Gamma_{ij1\dots n}(\mathbf{k}, \mathbf{k}', \mathbf{k}_1, \dots, \mathbf{k}_n) \chi_j(\mathbf{k}')^{-1} \int d\omega' G_{jl}(-\mathbf{q}') \\ = \Gamma_{ij1\dots n}(\mathbf{k}, \mathbf{k}', \mathbf{k}_1, \dots, \mathbf{k}_n) \delta_{jl} \delta(\mathbf{k}' + \mathbf{k}_l) \tag{A30}$$

which is just the negative of the value of the graph 5(d) containing a type *C* vertex (see the relation between the type *A* and *C* vertices in Fig. 4).

*Rule 4.* A graph in which one of the vertices [at position I in Fig. 5(e)] is connected to a second vertex by a loop as shown in Fig. 5(e) is canceled by another graph containing a type *B* vertex at position I shown in Fig. 5(f). The value of graph 5(e) is

$$\Gamma_{ij1\dots n}(\mathbf{k}, \mathbf{k}', \mathbf{k}_1, \dots, \mathbf{k}_n) \chi_j(\mathbf{k}')^{-1} \hat{G}_{ai}(\mathbf{q}) G_{bj}(\mathbf{q}') \Phi, \tag{A31}$$

where  $\Phi$  contains all the other factors due to the  $\gamma$  type legs. Since the vertex I represents interactions at earlier time than vertex II, the above expression can be rewritten as

$$\Gamma_{ij1\dots n}(\mathbf{k}, \mathbf{k}', \mathbf{k}_1, \dots, \mathbf{k}_n) \hat{G}_{ai}(\mathbf{q}) \hat{G}_{bj}(\mathbf{q}') \Phi \tag{A32}$$

which is the negative of the value of a similar graph with a type *B* vertex shown in Fig. 5(f) (see the relation between type *A* and *B* vertices in Fig. 4). This rule is applicable even

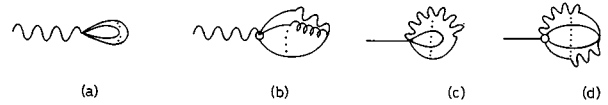


FIG. 6. Types of diagrams that are identically zero due to Rules 1 to 6 in the Appendix.

when the vertex at position II is a renormalized vertex, because it is always possible to choose the vertex at position I to have the earliest time index.

*Rule 5.* A vertex of type *A* in which the  $\alpha$  and  $\beta$  legs are directed towards increasing time [Fig. 5(g)] is canceled by a vertex of type *B* shown in Fig. 5(h). This rule can be easily verified in a manner similar to Rule 4. A graph with a type *A* vertex where the  $\beta$  leg is directed towards decreasing time is not canceled by a type *B* vertex because the latter is zero due to Rule 2.

*Rule 6.* A graph containing a loop with opposing  $\beta$  vertices as shown in Fig. 5(i) is canceled by two other graphs with type *B* vertices shown in Fig. 5(j) and 5(k). Here, we have used three relations in Figs. 5(i), 5(j) and 5(k)

$$G_{ia}(\mathbf{q}) \chi_a(\mathbf{k})^{-1} G_{jb}(\mathbf{q}') \chi_j(\mathbf{k}')^{-1} \\ = \hat{G}_{ia}(\mathbf{q}) \hat{G}_{jb}(\mathbf{q}') \chi_j(\mathbf{k}')^{-1} \chi_b(\mathbf{k}') + \hat{G}_{ai}(-\mathbf{q}) \\ \times \chi_a(\mathbf{k})^{-1} \chi_i(\mathbf{k}') \hat{G}_{bj}(-\mathbf{q}'), \\ \hat{G}_{ia}(\mathbf{q}) G_{jb}(\mathbf{q}') \chi_j(\mathbf{k}')^{-1} \\ = \hat{G}_{ia}(\mathbf{q}) \hat{G}_{jb}(\mathbf{q}') \chi_j(\mathbf{k}')^{-1} \chi_b(\mathbf{k}'), \\ \hat{G}_{bj}(-\mathbf{q}') G_{ai}(-\mathbf{q}) \chi_a(\mathbf{k})^{-1} \\ = \hat{G}_{bj}(-\mathbf{q}') \hat{G}_{ai}(-\mathbf{q}) \chi_a(\mathbf{k})^{-1} \chi_i(\mathbf{k}'). \tag{A33}$$

Using the above relations, as well as the fact that the coefficient of the type *B* vertex is the negative of that of the type *A* vertex (see Fig. 4), it can be easily verified that the sum of the three diagrams 5(i), 5(j), and 5(k) is zero. Rule 6 is also valid for renormalised vertices of the type shown in Fig. 5(l) if we take the leg  $b$  to be the one with the earliest time index on side I that is connected to a  $\beta$  leg on side II, and leg  $i$  to be the one with the earliest time index on side II that is connected to a  $\beta$  leg on side I.

Using these rules, it is quite easy to show that the stationarity condition (A25) is identically satisfied. The self-energy for the average  $\psi_i$  and  $\hat{\psi}_i$  consists of “tadpole” diagrams as shown in Fig. 6. All tadpole diagrams involving bubbles of the type in Fig. 6(a) are identically zero because of Rule 3, while those containing loops as in Fig. 6(b) are zero because of Rule 4. The tadpole diagrams for  $\hat{\psi}_i$  involving bubbles [Figs. 6(c) and 6(d)] are zero due to causality (Rule 1 and 2). Therefore, the Langevin equation (A3) coupled with a causal discretization scheme satisfies the stationarity condition.

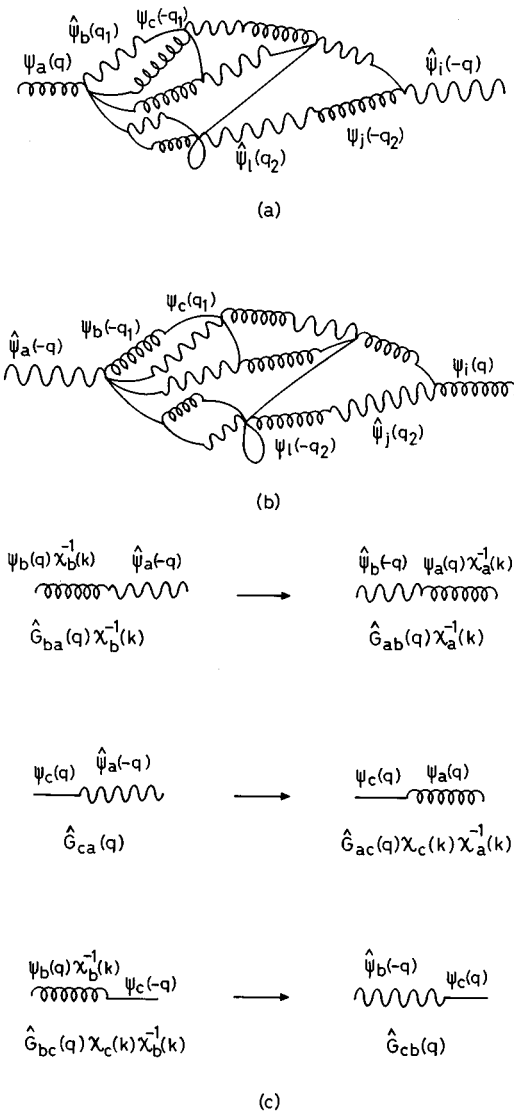


FIG. 7. Diagrammatic representation of the Onsager reciprocal relations.

Next, we consider the consistency conditions for the Onsager reciprocal relations (A28). The graph for the self energy  $\hat{\Sigma}_{ij}$  is a “tree”<sup>28</sup> with side bubbles of the type shown in Fig. 7(a). Note that all diagrams with side loops are zero by Rule 4, and so all the vertices have to be positioned along the main tree. In this, all the  $\alpha$  type legs are directed towards increasing time, and the  $\beta$  type legs are constrained to lie along the main tree due to Rule 3, and directed towards decreasing time due to Rule 4. The value of the diagram 7(a) can be written compactly as

$$\hat{\Sigma}_{ia}(\mathbf{q}) = \Gamma_{ba\dots}(-\mathbf{k}_1, -\mathbf{k}, \dots) \chi_a(\mathbf{k})^{-1} \Gamma_{ij\dots}(\mathbf{k}, \mathbf{k}_2, \dots) \Phi. \quad (\text{A34})$$

For every diagram of the type shown in Fig. 7(a), there exists another of the type in Fig. 7(b) where the positions of the  $\alpha$  and  $\beta$  legs are interchanged, all wave vectors are transformed as  $\mathbf{k}_i \rightarrow -\mathbf{k}_i$  and time progresses in the opposite direction (in

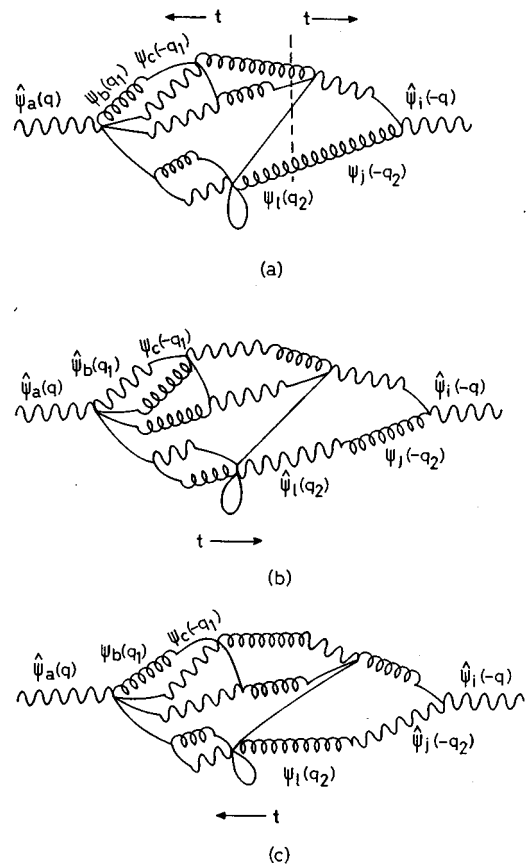


FIG. 8. Diagrammatic representation of the fluctuation–dissipation theorem.

effect,  $\mathbf{q}_i \rightarrow -\mathbf{q}_i$ ). Under this transformation, the propagators containing type  $\alpha$ ,  $\beta$  and  $\gamma$  legs are transformed as follows [see Fig. 7(c)]

$$\begin{aligned} \hat{G}_{ba}(\mathbf{q}) \chi_b^{-1}(\mathbf{k}) &\rightarrow \hat{G}_{ab}(\mathbf{q}) \chi_a^{-1}(\mathbf{k}), \\ \hat{G}_{ca}(\mathbf{q}) &\rightarrow \chi_a(\mathbf{k})^{-1} G_{ac}(\mathbf{q}) = \chi_a(\mathbf{k})^{-1} \hat{G}_{ac}(\mathbf{q}) \chi_c(\mathbf{k}), \\ \chi_b^{-1}(\mathbf{k}) G_{bc}(\mathbf{q}) &= \chi_b^{-1}(\mathbf{k}) \hat{G}_{bc}(\mathbf{q}) \chi_c(\mathbf{k}) \rightarrow \hat{G}_{cb}(\mathbf{q}). \end{aligned} \quad (\text{A35})$$

In the above equation, the correlation function involving a type  $\beta$  leg,  $G_{bc}(\mathbf{q})$  has been replaced by  $\hat{G}_{bc}(\mathbf{q}) \chi_c(\mathbf{k})$  because the  $\beta$  leg is directed towards decreasing time. Further, the above transformation also changes the vertices  $\Gamma_{ij\dots}$  as follows:

$$\begin{aligned} \Gamma_{ij1\dots n}(\mathbf{k}, \mathbf{k}', \mathbf{k}_1, \dots, \mathbf{k}_n) \\ \rightarrow \Gamma_{ji1\dots n}(-\mathbf{k}', -\mathbf{k}, -\mathbf{k}_1, \dots, -\mathbf{k}_n). \end{aligned} \quad (\text{A36})$$

It can be easily verified from Eq. (A21) that the values of all the response and correlation functions on the right and left side of Eq. (A35) are unchanged by the above transformation, and Eq. (A29) shows that the values of the vertices  $\Gamma_{ij\dots}$  in Eq. (A36) also remain unchanged. Therefore, the factor  $\Phi$  due to the internal vertices and propagators remains unchanged due to the transformation, and the self energy for the diagram in Fig. 7(b) is

$$\hat{\Sigma}_{ai}(\mathbf{q}) = \Gamma_{ab\dots}(\mathbf{k}, \mathbf{k}_1, \dots) \Gamma_{ji\dots}(-\mathbf{k}_2, -\mathbf{k}, \dots) \chi_i(\mathbf{k})^{-1} \Phi. \quad (\text{A37})$$

Thus there is a one-to-one correspondence between the diagrams for  $\hat{\Sigma}_{ai}(\mathbf{q})$  and  $\hat{\Sigma}_{ia}(\mathbf{q})$ , and from Eqs. (A34) and (A37) it can be seen that the following Onsager reciprocal relation is identically satisfied at all orders in perturbation theory:

$$\hat{\Sigma}_{ai}(\mathbf{q})\chi_i(\mathbf{k}) = \hat{\Sigma}_{ia}(\mathbf{q})\chi_a(\mathbf{k}). \quad (\text{A38})$$

This completes the proof of the Onsager reciprocal relations (A28).

Finally, we come to the fluctuation dissipation theorem (A28). The self-energy  $\Sigma_{ai}$  has a double tree structure,<sup>28</sup> joined by at least two  $\beta$  type legs from opposite directions as shown in Fig. 8(a). The internal vertices along the two trees are all type *A* vertices; type *B* vertices cancel other type *A* vertices according to Rule 5. Moreover, all diagrams involve a loops of the kind shown in Fig. 5(l), and therefore the total contributions of these diagrams is zero. However, type *B* vertices can be placed at the terminal positions, and typical diagrams obtained in this manner, involving the same vertices as Figs. 7(a) and 7(b), are shown in Figs. 8(b) and 8(c). The contribution of the diagram Fig. 8(b) that is not canceled by another diagram with a terminal type *A* vertex is

$$\Sigma_{ia}(\mathbf{q}) = -\Gamma_{ba\dots}(-\mathbf{k}_1, -\mathbf{k}, \dots)\Gamma_{ij\dots}(\mathbf{k}, \mathbf{k}_2, \dots)\Phi, \quad (\text{A39})$$

where the factor  $\Phi$  is the same as that in Eq. (A34). The diagram in Fig. 8(c) has the same structure as that in Fig. 7(c), though the wave vectors and frequencies are transformed as  $\mathbf{q} \rightarrow -\mathbf{q}$ . The value of this diagram is

$$\Sigma_{ia}(\mathbf{q}) = -\Gamma_{ab\dots}(-\mathbf{k}, -\mathbf{k}_1, \dots)\Gamma_{ji\dots}(\mathbf{k}_2, \mathbf{k}, \dots)\Phi^*, \quad (\text{A40})$$

where  $\Phi^*$  is the complex conjugate of  $\Phi$ , and is obtained by the transforming all wave vectors and frequencies  $\mathbf{q} \rightarrow -\mathbf{q}$  in Eq. (A37) [Fig. 7(b)]. Comparing Eqs. (A34), (A37), (A39),

and (A40), it can be easily verified that the fluctuation dissipation theorem (A27) is satisfied at each order in perturbation theory.

- <sup>1</sup>P. G. DeGennes, J. Chem. Phys. **72**, 4756 (1980).
- <sup>2</sup>P. Pincus, J. Chem. Phys. **75**, 1996 (1981).
- <sup>3</sup>K. Binder, J. Chem. Phys. **79**, 6387 (1983).
- <sup>4</sup>J. W. Cahn and J. E. Hilliard, J. Chem. Phys. **28**, 258 (1958).
- <sup>5</sup>J. W. Cahn and J. E. Hilliard, J. Chem. Phys. **31**, 668 (1958).
- <sup>6</sup>H. E. Cook, Acta Metall. **18**, 297 (1970).
- <sup>7</sup>J. S. Langer, H. D. Bar-on, and M. Miller, Phys. Rev. A **11**, 1417 (1975).
- <sup>8</sup>F. S. Bates and G. H. Fredrickson, Annu. Rev. Phys. Chem. **41**, 525 (1990).
- <sup>9</sup>L. Leibler, Macromolecules **13**, 1602 (1980).
- <sup>10</sup>G. H. Fredrickson and E. Helfand, J. Chem. Phys. **89**, 5890 (1988).
- <sup>11</sup>E. Helfand and Z. R. Wasserman, Macromolecules **9**, 879 (1976).
- <sup>12</sup>A. N. Semenov, Soviet Phys. JETP **61**, 733 (1985).
- <sup>13</sup>G. H. Fredrickson and E. Helfand, J. Chem. Phys. **93**, 2048 (1990).
- <sup>14</sup>J.-L. Barrat and G. H. Fredrickson, Macromolecules **27**, 832 (1992).
- <sup>15</sup>E. I. Shakhnovich and A. M. Gutin, J. Phys. (Paris) **50**, 1843 (1989).
- <sup>16</sup>G. H. Fredrickson and S. T. Milner, Phys. Rev. Lett. **67**, 835 (1991).
- <sup>17</sup>G. H. Fredrickson, S. T. Milner, and L. Leibler, Macromolecules **25**, 6341 (1992).
- <sup>18</sup>V. Kumaran and G. H. Fredrickson, Physica A **204**, 378 (1994).
- <sup>19</sup>E. D. Siggia, B. I. Halperin, and P. C. Hohenberg, Phys. Rev. B **13**, 2110 (1976).
- <sup>20</sup>P. C. Hohenberg and B. I. Halperin, Rev. Mod. Phys. **49**, 435 (1977).
- <sup>21</sup>N. van Kampen, *Stochastic Processes in Physics and Chemistry* (North-Holland, New York, 1981).
- <sup>22</sup>R. L. Stratonovich, *Topics in the Theory of Random Noise* (Gordon-Breach, New York, 1963).
- <sup>23</sup>G. Odian, *Principles of Polymerisation* (Wiley-Interscience, New York, 1981).
- <sup>24</sup>P.-G. de Gennes, *Scaling concepts in Polymer Physics* (Cornell University, New York, 1991).
- <sup>25</sup>R. V. Jensen, J. Stat. Phys. **25**, 183 (1981).
- <sup>26</sup>H. K. Janssen, Z. Phys. B **23**, 377 (1976).
- <sup>27</sup>R. Phythian, J. Phys. A **10**, 777 (1977).
- <sup>28</sup>U. Dekker and F. Haake, Phys. Rev. A **11**, 2043 (1975).